# Diaphragmatic morphological *post-mortem* findings in critically ill COVID-19 patients: an observational study

Luigi Vetrugno,[1,2] Cristian Deana,[3] Savino Spadaro,[4,5] Gianmaria Cammarota,[6,7] Domenico Luca Grieco,[8,9] Annarita Tullio,[10] Tiziana Bove,[3,11] Carla Di Loreto,[11,12] Salvatore Maurizio Maggiore,[2,13] Maria Orsaria,[12] the DIASUS Study Group*

Correspondence: Luigi Vetrugno, Department of Medical, Oral and Biotechnological Sciences, University of Chieti-Pescara, Via dei Vestini n 33, Chieti, 66100, Italy.
E-mail: luigi.vetrugno@unich.it

Key words: COVID-19, invasive mechanical ventilation, diaphragm dysfunction, myosin, ventilation-induced diaphragm injury.

Contributions: LV, was involved in the conception of the study, hypothesis generation, data analysis, writing and revision of the article before submission; CD, was involved in data collection, data analysis, writing and revision of the article before submission; SS, GMC, DLG, SMM, were involved in data analysis, writing and revision of the article before submission; AT, was involved in data analysis and took responsibility for it, writing and revision of the article before submission; DO, FM, were involved in data collection and writing article before submission; FB, TB, CDL, GV, were involved in data analysis, writing and revision of the article before submission; MO, was involved in the conception of the study, anatomo-pathological data curation, data analysis, writing and revision of the article before submission. All authors read and approved the final version of this manuscript. LV and CD share first authorship.

Conflict of interest: the authors declare that they have no competing interests

Ethics approval and consent to participate: the study was approved by the Institutional Review Board of the University of Udine (IRB ID 086/2021, November 22, 2021). Consent to participation was waived due to the retrospective design of the study.

Informed consent: for research purposes, it was obtained through general informed consent (GE.CO) signed at the time of hospital admission.

Patient consent for publication: consent to participation was waived due to the retrospective design of the study.

Availability of data and materials: data and materials are available from the corresponding author upon reasonable request.

Funding: none.

Received: 20 October 2023.
Accepted: 18 March 2024.
Early view: 23 April 2024.


*Monaldi Archives for Chest Disease 2025; 95:2829*
*doi: 10.4081/monaldi.2024.2829*



[1]Department of Medical, Oral and Biotechnological Sciences, Gabriele d'Annunzio University of Chieti Pescara, Chieti; [2]Department of Anesthesiology, Critical Care Medicine and Emergency, Annunziata Hospital, Chieti; [3]Department of Anesthesia and Intensive Care, Health Integrated Agency Friuli Centrale, Academic Hospital of Udine; [4]Department of Translational Medicine, University of Ferrara; [5]Intensive Care Unit, Azienda Ospedaliera Universitaria Sant'Anna, Ferrara; [6]Department of Translational Medicine, Università degli Studi del Piemonte Orientale, Novara; [7]Department of Anesthesiology and Intensive Care, Azienda Ospedaliero-Universitaria "Maggiore della Carità", Novara; [8]Department of Emergency, Intensive Care Medicine and Anesthesia, Fondazione Policlinico Universitario A. Gemelli IRCCS, Rome; [9]Department of Anesthesiology and Intensive Care Medicine, Catholic University of The Sacred Heart, Rome; [10]Health Integrated Agency Friuli Centrale, Academic Hospital of Udine; [11]Department of Medicine, University of Udine; [12]Institute of Anatomic Pathology, Health Integrated Agency Friuli Centrale, Academic Hospital of Udine; [13]Department of Innovative Technologies in Medicine and Dentistry, Gabriele d'Annunzio University of Chieti Pescara, Chieti, Italy

## Abstract

Our study investigates the *post-mortem* findings of the diaphragm's muscular structural changes in mechanically ventilated COVID-19 patients. Diaphragm samples of the right side from 42 critically ill COVID-19 patients were analyzed and correlated with the type and length of mechanical ventilation (MV), ventilatory parameters, prone positioning, and use of sedative drugs. The mean number of fibers was 550±626. The cross-sectional area was 4120±3280 μm², while the muscular fraction was 0.607±0.126. The overall population was clustered into two distinct populations (clusters 1 and 2). Cluster 1 showed a lower percentage of slow myosin fiber and higher fast fiber content than cluster 2 (68% *vs.* 82%, p<0.00001, and 29.8% *vs.* 18.8%, p=0.00045, respectively). The median duration of MV was 180 (41-346) hours. In cluster 1, a relationship between assisted ventilation and fast myosin fiber percentage ($R^2$=-0.355, p=0.014) was found. In cluster 2, fast fiber content increased with increasing length of the controlled MV ($R^2$=0.446, p=0.006). A high grade of fibrosis was reported. Cluster 1 was characterized by fibers' atrophy and cluster 2 by hypertrophy, supposing different effects of ventilation on the diaphragm but without excluding a possible direct viral effect on diaphragmatic fibers.

## Introduction

During spontaneous breathing, the main respiratory muscle, the diaphragm, generates a negative pressure permitting the air to penetrate the lungs and fill their space [1,2]. During noninvasive and invasive ventilation, the diaphragm can be partially assisted or fully supported during acute respiratory failure [3].

However, in animal models, these supportive strategies resulted in oxidation of diaphragmatic proteins and increased diaphragmatic proteolysis due to elevated protease activity with consequent diaphragmatic damage. A selective down-regulation of myosin has been found to be concurrent with accelerated protein degradation by the ubiquitin-proteasome pathway [4].

Similarly, Levine *et al*. demonstrated in a small subset of 14 brain-injured patients that diaphragmatic atrophy during mechanical ventilation (MV) is sustained by the activation of the ubiquitin-proteasome pathway [5].

Diaphragm atrophy and the potential onset of diaphragm weakness could culminate in ventilation-induced diaphragm dysfunction (VIDD) [6,7].

Other important risk factors associated with diaphragm weakness besides MV are the contemporary presence of sepsis, systemic inflammatory syndrome, or the use of some medications, especially sedatives, steroids, and muscle relaxant agents [8]. In non-COVID-19 patients, VIDD has a strong impact on clinical outcomes and is associated with difficult and prolonged weaning and extubation failure [9]. These consequences increase morbidity and mortality in critically ill patients [10].

It is unknown whether critically ill COVID-19 patients who underwent MV experienced VIDD as the consequence of ventilation per se or as a direct effect of the virus, as recently shown by Shi *et al*. [11].

Moreover, a recent study evaluating 50 patients previously hospitalized with COVID-19 (14 females, age 58±12 years, half treated with MV and half treated outside intensive care settings with non-invasive ventilation) showed that diaphragm muscle weakness was still present 15 months after hospitalization. Furthermore, diaphragm weakness was associated with dyspnea on exertion. In this study, the authors identified diaphragm muscle weakness correlated with persistent dyspnea [12].

Therefore, our study aims to explore the anatomopathological diaphragm changes in COVID-19 intensive care unit (ICU) patients after MV.

## Materials and Methods

### Study protocol and design

This study was an observational *post-mortem* study of COVID-19 patients admitted to the ICU who underwent invasive MV due to acute respiratory failure. The study was registered on ClinicalTrialsl.gov on January 13, 2022 (NCT05191433), after obtaining approval from the Institutional Review Board of the University of Udine (IRB ID 086/2021, November 22, 2021). This study follows STROBE reporting guidelines for observational studies.

### Study population

Inclusion criteria were: i) adult mechanically ventilated patients aged 18 years and above; ii) deceased from SARS-CoV-2 pneumonia in the ICU who underwent *post-mortem* pathological examination. Exclusion criteria were: i) ventilated COVID-19 patients with a life expectancy <48 hours; ii) COVID-19 positive patients admitted to the ICU with do-not-intubate or do-not-resuscitate orders; iii) severe end-stage organ disease (patients awaiting liver or heart, or kidney transplantation, patients under chronic hemodialysis); iv) extracorporeal membrane oxygenator support.

### Recorded patient data

Anthropometric data such as gender, age, weight, height, and body mass index (BMI), previous medical history were recorded, as well as length of MV and length of stay in the ICU ($ICU_{LOS}$).

### Pathology examination

All our institution's pathologists used the same protocol when performing *post-mortem* examinations of patients who died from SARS-CoV-2 infection. Diaphragm sampling was performed on the right side of the diaphragm at a distance of 2-3 cm from the costal insertion, approximately 24 hours after the *post-mortem* period. This area corresponds to the one explored with ultrasound and is known as the zone of apposition. The portion of tissue obtained was then dissected and placed in Sakura Tissue-Tek Para form Sectionable Cassettes (Sakura Finetek Europe B.V., Mestre, Italy) according to various cutting planes to increase the probability of getting cross-sections of muscle fibres. The sample preparations were then processed, included in paraffin, and, from each block, sections were cut and later stained with hematoxylin-eosin. The resulting slides were scanned and acquired using a Leica Aperio AT2 slide scanner at 40× (Leica Biosystems, Milan, Italy).

Digital slides were then uploaded to the Omero Server (©2005-2022 Glencoe Software, Inc.), where a pathologist annotated one or more regions of interest (ROI) per slide, choosing the points where the muscle fibres appeared to be cut transversely and with a rounded shape, avoiding picking those deformed or with an incorrect cutting plane (Figure 1a and b).

Such regions were exported in TIFF format images for further data processing. Quantitative evaluation was carried out using a macro script for the ImageJ image analysis software (National Institutes of Health, USA, 2020). The muscle fibres were hand-selected based on color, excluding the smallest regions (possibly due to noise or non-muscle tissue). To evaluate the fibre sections, a filter based on the shape circularity was also used to discharge regions with more than one fibre (which results in an irregular and vast region), as shown in Figure 1c. For each ROI, the software calculated the number of fibres, the cross-sectional area (CSA), the mean perimeter and the mean diameter of the fibres, and the muscle fraction over the total tissue examined.

### Immunohistochemical analysis

To define the fibre types, paraffin-embedded human skeletal muscle tissue labelling Slow Skeletal Myosin Heavy chain and Fast Myosin Skeletal Heavy chain +MYH4 was performed following Abcam antibody datasheet instructions (heat mediated antigen retrieval with Tris/EDTA buffer pH 9.0, use of clone ab234431 or clone ab255685, respectively, at 1/500 dilution), followed by a ready-to-use Rabbit specific IHC polymer detection kit HRP/DAB. The section was incubated with ab234431 for 30 minutes at room temperature. The immunostaining was performed on a Ventana instrument and counterstained with hematoxylin. Cytoplasmic positivity in the human skeletal muscle was obtained,

as shown in Figure 1d. Antibodies directed against slow and fast were performed in two consecutive slides, therefore distant approximately 3.5-4 mm from each other, a distance that could hardly differentiate significantly the fiber morphology, allowing us to superimpose the two slides.

## Ventilation parameters and intensive care unit treatments

We reported MV mode (pressure-controlled, volume-controlled, volume-guaranteed pressure-controlled, or pressure support ventilation), ventilation parameters [tidal volume ($V_T$), plateau pressure, end expiratory positive pressure, pressure support, fraction of inspired oxygen ($F_IO_2$), and blood gas analysis results (partial pressure of oxygen ($PaO_2$), partial pressure of carbon ($PaCO_2$), $PaO_2/F_IO_2$ ratio)]. The respiratory system driving pressure (DP), elastance ($E_L$), and mechanical power (MP) according to Guerin's method were computed whenever possible as follows: $0.098 \times V_T \times$respiratory rate (RR)$\times$DP [13]. Moreover, we used the recent simplified formula as suggested by Costa [(4×DP)+RR], which is as informative as MP [14]. Hemodynamic parameters (heart rate and mean arterial pressure), vasopressor use, sedation, muscle relaxants, pronation, and nitric oxide use were also recorded.

## Study outcomes

This study investigates the histopathologic *post-mortem* findings of the diaphragm in critically ill COVID-19 patients who underwent MV. As a secondary outcome, we investigated possible clusters of patients defined by different characteristics in pathology findings, if any. We finally explored potential correlations between pathology findings and the different modes of MV, prone position, nitric oxide administration, neuromuscular blocker use, and the effects of the sedative drugs.

## Statistical analysis

Continuous variables are expressed as mean and standard deviation, or median and minimum/maximum values, or interquartile ranges, where appropriate. Categorical variables are expressed as absolute numbers and percentages. The Student *t*-test or the Wilcoxon-Mann-Whitney test was used to compare continuous variables, based on Kolmogorov-Smirnov normality test results, and the $\chi^2$ analysis or the Fisher exact test for categorical variables, as appropriate based on expected frequencies.

We used the K-medoids clustering partitioning around medoids algorithm to cluster our population, including in the algo-

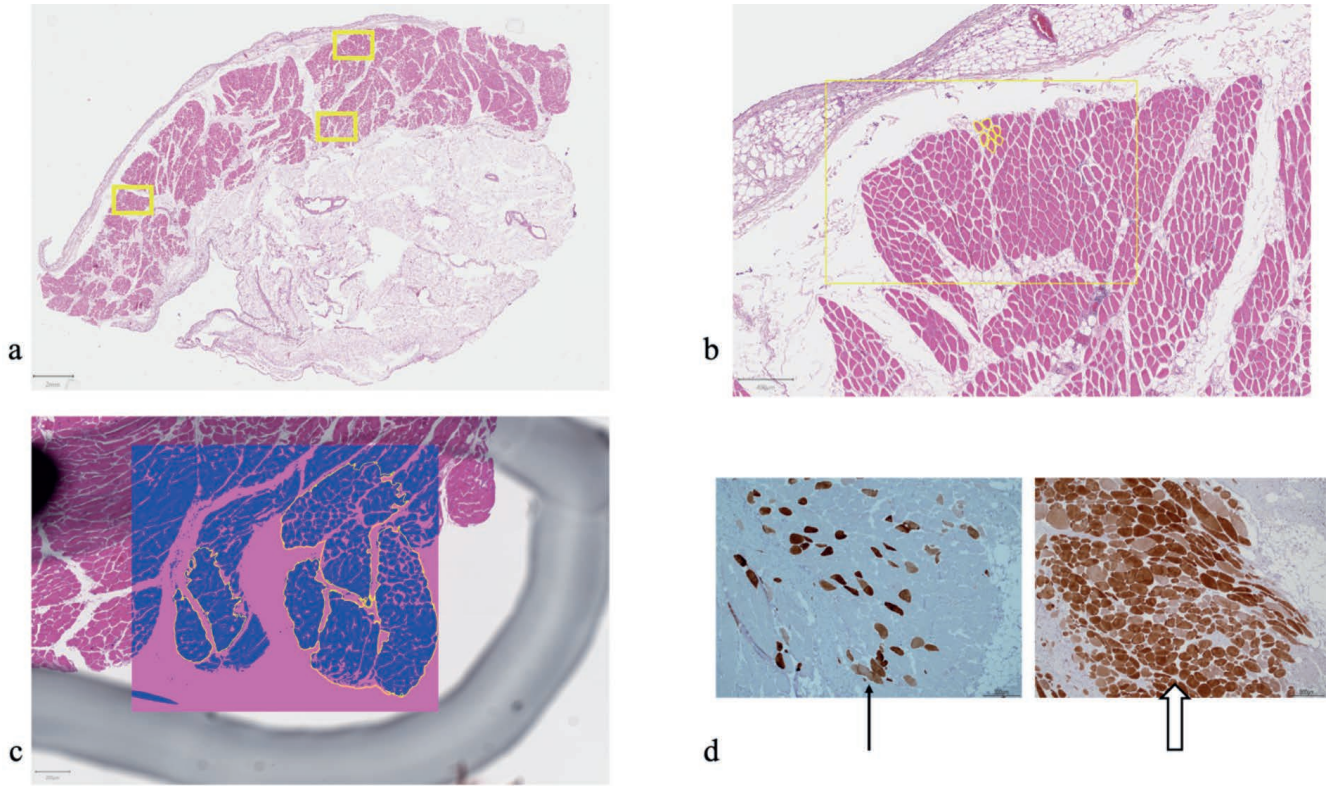


**Figure 1.** Diaphragm sections and digital acquisition of images. The diaphragm tissue slides were scanned and acquired using a Leica Aperio AT2 slide scanner at 40×. Digital slides were then uploaded to an Omero Server, where a pathologist annotated one or more regions of interest per slide (a). After that, the pathologist annotated the points where the muscle fibers appeared to be cut transversely and with a rounded shape, avoiding picking those that appeared deformed or with an incorrect cutting plane (b). Quantitative evaluation has been carried out by means of a macro script for the ImageJ image analysis software (c). The script selected the muscle fibers based on color, excluding the smallest regions (possibly due to noise or non-muscle tissue). For evaluating the fiber sections, a filter based on the shape circularity has also been used to discharge regions constituted by more than one fiber (which results in an irregular and very large region). The thin arrow shows slow skeletal myosin heavy chain cytoplasmic positivity (Abcam clone ab234431, 4×), while the black empty arrow points put fast skeletal myosin heavy chain cytoplasmic positivity (Abcam clone ab255685, 4×) (d). Antibodies directed against slow and fast were performed in two consecutive slides, therefore distant approximately 3.5-4 mm from each other, a distance that could hardly differentiate significantly the fiber morphology, allowing us to superimpose the two slides.

rithm the three most important anatomo-pathological variables (fast myosin, slow myosin, and the number of fibres). We used the average silhouette method to estimate the optimal number of clusters. The Wilcoxon-Mann-Whitney test was used to compare continuous variables between the two clusters, and the Fisher exact test was used to compare categorical variables between the two clusters. All these analyses were done in the overall population. However, to be more precise and to evaluate the potential relationship (with Pearson or Spearman's correlation test as appropriate) between anatomopathological findings and ventilatory parameters, we decided to include only patients with complete data regarding ventilatory parameters.

The sample size was calculated considering an expected difference of 500 $\mu m^2$ in CSA between groups 1 and 2 as the main objective.

Assuming a pooled standard deviation of 470 $\mu m^2$, we have calculated a sample size of 14 for each group (*i.e.*, a total sample size of 28, assuming equal group sizes), to achieve a power of 80% and a level of significance of 5% (two sided), for detecting a true difference in means between group 1 and 2 of 500 (*i.e.*, 3000-2500) $\mu m^2$.

All statistical analyses were performed using R software version 4.0.2 (R Core Team 2020, Vienna, Austria). Figures reporting correlations were made with the GraphPad Prism version 9.4.1. The significance level was set at 0.05. No imputation was done for missing data.

## Results

From November 1st, 2020, to March 30th, 2021, we studied 42 patients. They were mainly men (83%), 70 (66-76) years old, with a BMI of 27.8 (25.4-31.2) $kg/m^2$. Previous medical history is furnished in *Supplementary Table 1*. Median duration of MV was 180 (41-346) hours. Moreover, median $ICU_{LOS}$ was 240 hours (96-396), corresponding to 10 days.

The overall population showed a higher percentage of slow than fast fibres, 74.4% and 24.8%, respectively. The mean number of fibres in the ROIs investigated was 550±626. The CSA of fibres was 4120±3280 $\mu m^2$. Mean perimeter was 274±111 µm, while maximum diameter was 93±37.8 µm. The muscular fraction (area occupied by muscle fibres over total area analyzed) was 0.607±0.126.

According to the partition analysis described in the methods section, we detected two clusters, dividing the population into cluster 1 (23 patients) and cluster 2 (19 patients). There were no significant differences in the baseline characteristics of the two clusters, as shown in *Supplementary Table 1*. They differed in the percentage of slow and fast myosin and the number of fibres in the ROIs investigated, as shown in Table 1.

When analyzing ventilation data, we included 29 patients, 14 belonging to cluster 1 and 15 in cluster 2.

A trend toward statistically significant difference was observed when comparing cluster 1 *vs*. cluster 2 regarding the percentage of

**Table 1.** Biopsy findings and comparison between clusters.

| | Overall (n=42) | Cluster 1 (n=23) | Cluster 2 (n=19) | p |
|---|---|---|---|---|
| Slow myosin % | 74.4 (9.7) | 68.3 (7.01) | 81.8 (6.91) | *<0.00001* |
| Fast myosin % | 24.8 (10.2) | 29.8 (7.30) | 18.8 (10.2) | *0.00045* |
| N° fibers | 550 (626) | 790 (756) | 259 (182) | *0.00030* |
| CSA ($\mu m^2$) | 4120 (3280) | 3380 (2780) | 5010 (3680) | 0.07675 |
| Perimeter (µm) | 274 (111) | 248 (101) | 305 (118) | 0.06850 |
| Diameter (µm) | 93.0 (37.8) | 84.4 (33.6) | 103 (40.8) | 0.12407 |
| Muscle fraction | 0.607 (0.126) | 0.604 (0.141) | 0.611 (0.108) | 0.94953 |

Values are expressed as mean and standard deviation. CSA, cross-sectional area.

**Table 2.** Main intensive care unit data.

| | Overall (n=29) | Cluster 1 (n=14) | Cluster 2 (n=15) | p |
|---|---|---|---|---|
| Duration of MV (hours) | 180 (41-346) | 231 (102-425) | 167 (8-295) | 0.27 |
| NIV (% over total time of $ICU_{LOS}$) | 0 (0-0.04) | 0 (0-0.01) | 0.01 (0-0.1) | 0.23 |
| Controlled MV (% over total time of $ICU_{LOS}$) | 0.57 (0.30-0.70) | 0.59 (0.45-0.81) | 0.53 (0.17-0.59) | 0.06 |
| PSV (% over total time of $ICU_{LOS}$) | 0.12 (0-0.27) | 0.08 (0.03-0.31) | 0.18 (0-0.28) | 0.70 |
| Sedation (% over total time of $ICU_{LOS}$) | 0.88 (0.52-0.94) | 0.92 (0.77-0.96) | 0.81 (0.21-0.93) | 0.07 |
| Muscular paralysis (% over total time of $ICU_{LOS}$) | 0.18 (0-0.43) | 0.14 (0.025-0.42) | 0.27 (0-0.43) | 0.74 |
| Prone positioning (% over total time of $ICU_{LOS}$) | 0.04 (0-0.12) | 0.09 (0-0.14) | 0.03 (0-0.11) | 0.36 |
| iNO (% over total time of $ICU_{LOS}$) | 0 (0-0.15) | 0 (0-0.20) | 0 (0-0.17) | 0.98 |
| $PaO_2$ (mmHg) | 75 (66-91) | 73.5 (66-90) | 77 (66-91) | 0.74 |
| $PaCO_2$ (mmHg) | 45 (39-54) | 44 (38-51) | 48 (43-66) | 0.11 |
| $PaO_2/FIO_2$ (mmHg) | 128 (100-178) | 136 (93-257) | 115 (100-145) | 0.34 |
| MAP (mmHg) | 77 (68-90) | 82 (70-93) | 71 (65-84) | 0.10 |
| HR (bpm) | 71 (60-87) | 64 (50-74) | 74 (70-100) | 0.001 |

Data are expressed as median and (interquartile ranges). MV, invasive mechanical ventilation; ICU, intensive care unit; NIV, noninvasive ventilation; PSV, pressure support ventilation; $ICU_{LOS}$, ICU length of stay; iNO, nitric oxide; $PaO_2$, partial pressure of oxygen; $PaCO_2$, partial pressure of carbon dioxide; $PaO_2/F_1O_2$, partial pressure of oxygen/fraction of inspired oxygen; MAP, mean arterial pressure; HR, heart rate.

time spent under controlled MV and sedation during ICU stay, 59% *vs.* 53%, p=0.06, and 92% *vs.* 81%, p=0.07, respectively, as shown in Table 2.

As reported in Table 3, $V_T$, DP, and $E_L$ of the respiratory system were similar in clusters 1 and 2 (p=0.90 for tidal volume, p=0.07 for DP, and p=0.11 for $E_L$). On the contrary, MP was lower in cluster 1 than cluster 2, 17.2 *vs.* 21.4 J/min (p=0.03), respectively. Similarly, the results of Costa's formula were 95 *vs.* 107 in cluster 1 and cluster 2, respectively (p=0.009).

A weak positive correlation was observed in the overall population between the time spent under controlled MV and the percentage of fast myosin fibres ($R^2$=0.156, p=0.034). Similarly, the longer the time under pronation, the higher the muscle fibres' fraction ($R^2$=0.197, p=0.017).

Analyzing the relationship between ventilatory data and anatomopathological characteristics in the two clusters separately, we found a negative relationship between the time spent under assisted ventilation and the percentage of fast myosin fibres ($R^2$=-0.355, p=0.014) in cluster 1. On the contrary, cluster 2 showed a direct positive linear relationship between the same parameters ($R^2$=0.246, p=0.059). In cluster 2, the percentage of fast fibres increased with increasing the amount of time spent under controlled MV ($R^2$=0.446, p=0.006). Number per micron was reduced for prolonged periods of controlled MV ($R^2$=-0.34, p=0.022) (*Supplementary Figure 1*). No correlation was found for the same variables in cluster 1. A negative correlation between the number of muscular fibres and the total length of MV ($R^2$=-0.293, p=0.037) was found in cluster 2.

Inverse correlation between mean tidal volume and the percentage of fast myosin fibres was found in cluster 1 ($R^2$=-0.37, p=0.022). On the contrary, the same correlation was positive in cluster 2 ($R^2$=0.312, p=0.046) as shown in Figure 2. A direct positive correlation between the $PaO_2/F_IO_2$ ratio and the number of fibres was found only in cluster 1 ($R^2$=0.514, p=0.004). MP demonstrated a negative linear correlation with the percentage of fast fibres in cluster 1 ($R^2$=-0.459, p=0.031). MP and Costa's formula demonstrated a positive linear correlation ($R^2$=0.67, p<0.0001). All comparisons between ventilatory and anatomopathological correlations are available as *Supplementary Table 2*.

## Discussion

The main findings in the present study are i) in mechanically ventilated critically ill COVID-19 patients, slow muscular fibres are predominant over fast fibres; ii) extracellular components represented 40% of ROIs investigated; iii) based on anatomopathological findings, two distinct clusters of patients could be described, where cluster 1 is characterized mainly by atrophy of the diaphragm, and cluster 2 is characterized by hypertrophy of diaphragmatic muscular fibres; iv) there was a different relationship between anatomopathological findings and ventilation features within the clusters; in particular in cluster 1, fast fibres decreased with increased time under assisted ventilation and tidal volume; in cluster 2, a positive correlation was found between fast fibre percentage and time under assisted ventilation and tidal volume.

Slow and fast fibres are usually in about equal proportions in the adult human diaphragm (about 55% slow fibres, 45% fast fibres) [15].

Jaber *et al*., in a small cohort of non-COVID critically ill patients after long-term (80 hours) and short-term (2 hours) MV for endoscopic digestive procedures with general anaesthesia, reported a preserved type 1 over type 2 fibre ratio close to 50% [6]. In our study, on the contrary, about 74% of fibres were represented by slow type (type I).

The unusually high percentage of fast MHC-positive fibers in comparison with the typical observation in non-COVID-19 patients could be explained as a response to the increased neural respiratory drive observed in these patients, which in turn increases the protein synthesis to sustain the work of breathing [16-18].

We also observed an increased rate of fibrosis that reached about 40% of the tissue examined, since it usually occupies a proportion between 1-20% of human skeletal muscle [19].

Our results seem to confirm a previous study in COVID-19 ICU patients by Shi *et al*. [11]. In *post-mortem* diaphragm findings from three medical centers, they observed an increased expression of genes involved in fibrosis and histological evidence for the development of fibrosis in the diaphragm. This "myopathic phenotype" was different from that of control-ICU patients, considering comparable duration of MV and $ICU_{LOS}$. The authors could not establish whether diaphragm myopathy is a direct effect of SARS-CoV-2 [11].

However, it is probable that not all patients develop the same diaphragmatic alterations. We identified two different clusters of patients considering the anatomopathological findings: cluster 1 showed atrophy of the diaphragm, while cluster 2 patients were more likely to show hypertrophy.

The structural and functional characteristics of respiratory muscle fibres are not fixed, and can be modified in response to

**Table 3.** Ventilation parameters.

| | Overall (n=29) | Cluster 1 (n=14) | Cluster 2 (n=15) | p |
|---|---|---|---|---|
| Pplateau ($cmH_2O$) | 34 (30-35) | 32 (28-34) | 34 (30-36) | 0.15 |
| PEEP ($cmH_2O$) | 12 (10-14) | 12 (10-14) | 12 (10-14) | 0.76 |
| PS ($cmH_2O$) | 12 (10-13) | 12 (10-13) | 12 (10-14) | 0.80 |
| $F_IO_2$ (%) | 60 (50-80) | 55 (35-65) | 70 (60-80) | 0.02 |
| RR (apm) | 20 (17-21) | 20 (20-23) | 18 (19-22) | 0.07 |
| $V_T$ (mL/Kg IBW) | 6.8 (6.2-7.6) | 6.8 (6.2-7.6) | 6.7 (6.2-8) | 0.90 |
| ΔP ($cmH_2O$) | 20 (18-22) | 19.5 (17.7-21.0) | 22 (20-24) | 0.07 |
| EL ($cmH_2O$/L) | 38.2 (35.3-41.5) | 37.8 (34.5-39.5) | 39.3 (35.9-46.2) | 0.11 |
| MP (J/min) | 20.15 (16.1-22.8) | 17.2 (13.8-20.6) | 21.4 (17.9-26.1) | 0.03 |
| Costa's formula [(4 x DP) + RR] | 100 (94.5-107.5) | 95 (86.7-101.8) | 107 (98-114) | 0.009 |

Data are expressed as median and (interquartile ranges). $P_{plateau}$, plateau pressure; PEEP, end expiratory positive pressure; PS, pressure support; $F_IO_2$, fraction of inspired oxygen; RR, respiratory rate; $V_T$, tidal volume; IBW, ideal body weight; ΔP, driving pressure; $E_L$, elastance; MP, mechanical power.

several physiological and pathological conditions such as gender, training, age-related modifications, changes associated with pharmacological agents (a2-agonists and corticosteroids, for example) or hypoxia [19].

Training-induced hypertrophy increases the muscle fibre CSA and would result in a proportional increase in myofibrillar protein abundance, reported to happen through the addition of sarcomeres in series or parallel in existing myofibrils (*i.e*., sarcomerogenesis), or due to the synthesis of new myofibrils in existing muscle fibres (*i.e*., myofibrillogenesis) [20].

Given the composition of skeletal muscle, patients in cluster 2 probably developed a different kind of hypertrophy, not only caused by an increase in sarcomeres or myofibrils but also by connective tissue hypertrophy (due to an increase in the volume of the extracellular matrix that shows an increase in mineral or protein) [21].

One consideration should be explored at this point: it is possible that COVID-19 patients experience lengthy periods of silent hypoxemia with low arterial oxygen content, stimulating a high respiratory drive to increase oxygen delivery [22,23]. This can be considered an endurance-like stimulus during respiratory muscle recruitment, which could favour type 1 over type 2 fibres, considering the former are more suitable for sustained, prolonged workloads [24].

It has been shown that during controlled MV, the right and left hemidiaphragms undergo passive shortening during mechanical expansion of the lungs. In contrast, bilateral inactivity of the diaphragm, due to either nerve blockage or denervation, results in passive stretching of the inactivated diaphragm region during inspiration. This is significant within our context because it has been postulated that the transient hypertrophy of type 1 and 2a fibers in the rat diaphragm during bilateral denervation is due to increased protein synthesis induced by the passive stretch of the muscle during breathing [4,25]. Shortening of diaphragmatic adaptation to inactivity remains unknown; this is an interesting area for future research. Moreover, a high RR induces high respiratory loading, which is known to cause diaphragm myofibre injury [26].

In other words, critically ill COVID-19 patients appear more prone to developing fibrosis due to the direct stimulation of enzymes involved in the fibrogenic pathway, which could impair diaphragmatic performance [27]. However, appropriate respiratory support during the pandemic was guaranteed only in part due to the scarcity of ventilators and hospital reorganization [28]. Investigation of the diaphragm's function with ultrasound has been increasingly used [29,30].

Cammarota *et al*. have recently shown that the pronation of COVID-19 patients with C-ARDS can increase the diaphragmatic thickening fraction. The authors explain this process through the increased respiratory workload induced by the prone position, which is determined by reduced chest wall compliance [31]. In agreement with this hypothesis, we observed a positive linear correlation between the muscle/total tissue ratio increase and time

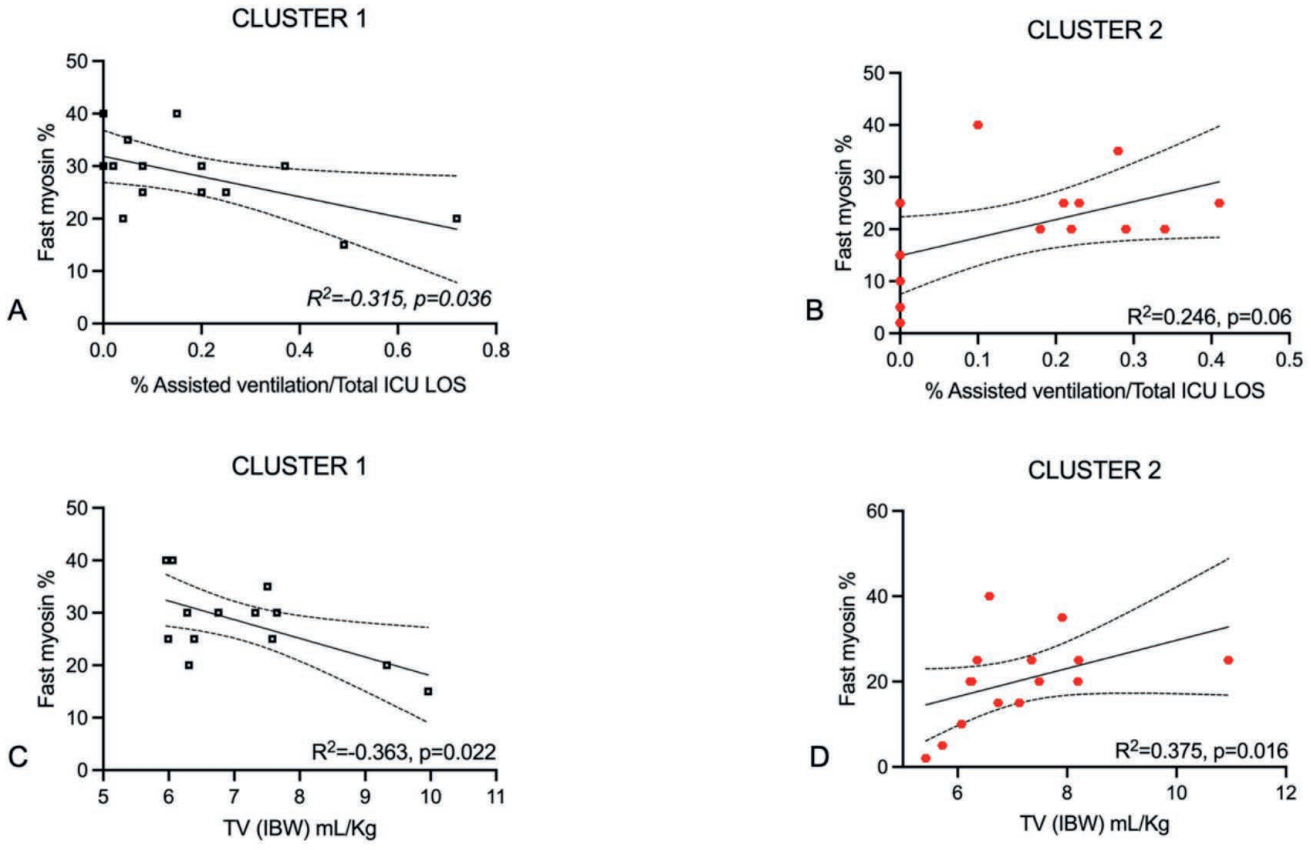


**Figure 2.** A) Fast fiber content relationship and ventilatory parameters within the two different clusters. Negative relationship between the time spent under assisted ventilation and the percentage of fast myosin fibres ($R^2$=-0.355, p=0.014) was found in cluster 1; B) on the contrary, cluster 2 showed a direct positive linear relationship for the same parameters ($R^2$=0.246, p=0.059); C) an inverse correlation between mean tidal volume and the percentage of fast myosin fibres was highlighted in cluster 1 ($R^2$=-0.37, p=0.022); D) on the contrary, the same correlation was positive in cluster 2 ($R^2$=0.312, p=0.046).

spent in the prone position in our COVID-19 patients in cluster 2.

In addition, the number of fibres in the same cluster (cluster 2) was reduced by increasing the duration of controlled MV. These results confirm that prolonged MV induces atrophy in the diaphragm [32].

We do not know if this change is directly affected by SARS-CoV-2 [12] or whether it is due to MV *per se*.

Similar results have been found by Hennigs *et al*. in a study where they described respiratory muscle dysfunction 5 months after COVID-19 infection across the spectrum of the disease, from mild to severe patterns [33].

These works are another piece of the puzzle about the complex interplay between the possible direct effect of the virus on the diaphragm and injury caused by MV.

Interestingly, in our study, assisted ventilation (pressure support) and the percentage of fast fibres demonstrated a very different correlation in cluster 1 compared to cluster 2. While in the former, the fast fibre percentage showed a reduction for longer assisted ventilation periods and higher $V_T$, an inverse correlation was found in the latter cluster.

MP demonstrated a negative linear correlation with the percentage of fast fibres in cluster 1; however, Costa's formula did not. As such, we argue that $V_T$, which was the only different variable between them, could play a possible role in determining this change in diaphragm structure.

MV *per se* alters diaphragm structure. However, the changes in the structural composition of respiratory muscles such as the diaphragm are probably due to multifactorial events: both the increase of the respiratory workload and the inflammation (during early phase) and the diaphragmatic dysfunction caused by MV, fibrogenesis processes (in the late phase) could be involved as common causes, leading to poor residual lung function [34,35]. Further genetic assessments related to the expression of type I and type II muscle fibres in critically ill COVID-19 patients might be useful.

This is an exploratory study aimed at evaluating changes induced by MV in the diaphragmatic musculature of critically ill COVID-19 patients. Our study carries some limitations. First, the limited sample size precludes any generalization of the results.

We have not evaluated additional variables that may be involved in the determinism of the changes mentioned above. In addition, we cannot assess the impact of different ventilation modes and settings beyond the observed changes in diaphragm structure. In addition, we cannot exclude a direct effect of the virus on diaphragmatic fibres since no comparison group (non-COVID-19 patients) has been studied.

Some limitations of CSA calculations by the microscopic assessment due to the method of tissue processing (*i.e*., climate of the laboratory, buffers, *etc*.), biopsy location (it is challenging to biopsy the exact location in a muscle), and measurement methods also need to be acknowledged. Moreover, the muscle can respond to training in a non-uniform manner (proximal *vs.* distal), which is difficult to appreciate in a single-site measurement.

Finally, we did not investigate the molecular pathway potentially related to gene expression, such as fibrogenic or hypertrophic pathways. However, this was beyond the aim of this study.

## Conclusions

In mechanically ventilated critically ill COVID-19 patients, fast myosin fibres were reduced, and extracellular components increased, with a net prevalence of slow fibres. This led us to describe two patient clusters: one in which atrophy prevailed and a second cluster in which hypertrophy was most prevalent. The MP instead of DP and the formula (4×DP)+RR were able to capture this ventilation-diaphragm interaction. These results need confirmation in prospective studies with a larger sample size, also in patients without COVID-19.

## References


1. McCool FD, Manzoor K, Minami T. Disorders of the diaphragm. Clin Chest Med 2018;39:345-60.
2. Doorduin J, van Hees HW, van der Hoeven JG, Heunks LM. Monitoring of the respiratory muscles in the critically ill. Am J Respir Crit Care Med 2013;187:20-7.
3. Telias I, Brochard LJ, Gattarello S, et al. The physiological underpinnings of life-saving respiratory support. Intensive Care Med 2022;48:1274-86.
4. Shanely RA, Zergeroglu MA, Lennon SL, et al. Mechanical ventilation-induced diaphragmatic atrophy is associated with oxidative injury and increased proteolytic activity. Am J Respir Crit Care Med 2002;166:1369-74.
5. Levine S, Nguyen T, Taylor N, et al. Rapid disuse atrophy of diaphragm fibres in mechanically ventilated humans. N Engl J Med 2008;358:1327-35.
6. Jaber S, Petrof BJ, Jung B, et al. Rapidly progressive diaphragmatic weakness and injury during mechanical ventilation in humans. Am J Respir Crit Care Med 2011;183:364-71.
7. Petrof BJ, Jaber S, Matecki S. Ventilator-induced diaphragmatic dysfunction. Curr Opin Crit Care 2010;16:19-25.
8. Dres M, Goligher EC, Heunks LMA, Brochard LJ. Critical illness-associated diaphragm weakness. Intensive Care Med 2017;43:1441-52.
9. Goligher EC, Dres M, Fan E, et al. Mechanical ventilation-induced diaphragm atrophy strongly impacts clinical outcomes. Am J Respir Crit Care Med 2018;197:204-13.
10. Frutos-Vivar F, Esteban A, Apezteguia C, et al. Outcome of reintubated patients after scheduled extubation. J Crit Care 2011;26:502-9.
11. Shi Z, de Vries HJ, Vlaar APJ, et al. Dutch COVID-19 diaphragm investigators. diaphragm pathology in critically ill patients with COVID-19 and postmortem findings from 3 medical centers. JAMA Intern Med 2021;181:122-4.
12. Regmi B, Friedrich J, Jörn B, et al. Diaphragm muscle weakness might explain exertional dyspnea 15 months after hospitalization for COVID-19. Am J Respir Crit Care Med 2023;207:1012-21.
13. Guérin C, Papazian L, Reignier J, et al. Effect of driving pressure on mortality in ARDS patients during lung protective mechanical ventilation in two randomized controlled trials. Crit Care 2016;20:384.
14. Costa ELV, Slutsky AS, Brochard LJ, et al. Ventilatory variables and mechanical power in patients with acute respiratory distress syndrome. Am J Respir Crit Care Med 2021;204:303-11.
15. Mizuno M. Human respiratory muscles: fibre morphology and capillary supply. Eur Respir J 1991;4:587-601.
16. Vetrugno L, Castaldo N, Fantin A, et al. Ventilatory associated barotrauma in COVID-19 patients: a multicenter observational case control study (COVI-MIX-study). Pulmonology 2022;29:457-68.
17. Vetrugno L, Orso D, Corradi F, et al. Diaphragm ultrasound evaluation during weaning from mechanical ventilation in COVID-19 patients: a pragmatic, cross-section, multicenter study. Respir Res 2022;23:210.

18. Cammarota G, Bruni A, Morettini G, et al. Lung ultrasound to evaluate aeration changes in response to recruitment maneuver and prone positioning in intubated patients with COVID-19 pneumonia: preliminary study. Ultrasound J 2023;15:3.
19. Polla B, D'Antona G, Bottinelli R, Reggiani C. Respiratory muscle fibres: specialisation and plasticity. Thorax 2004;59: 808-17.
20. Haun CT, Vann CG, Roberts BM, et al. A critical evaluation of the biological construct skeletal muscle hypertrophy: size matters but so does the measurement. Front Physiol 2019;10:247.
21. Roberts MD, Haun CT, Vann CG, et al. Sarcoplasmic hypertrophy in skeletal muscle: a scientific "unicorn" or resistance training adaptation?. Front Physiol 2020;11:816.
22. Dhont S, Derom E, Van Braeckel E, et al. The pathophysiology of 'happy' hypoxemia in COVID-19. Respir Res 2020;21:198.
23. Deana C, Verriello L, Pauletto G, et al. Insights into neurological dysfunction of critically ill COVID-19 patients. Trends in Anaesthesia & Critical Care 2021;36:30-8.
24. Reid WD, Belcastro AN. Time course of diaphragm injury and calpain activity during resistive loading. Am J Respir Crit Care Med 2000;162:1801-6.
25. Miyata H, Zhan WZ, et al. Myoneural interactions affect diaphragm muscle adaptations to inactivity. J Appl Physiol (1985) 1995;79:1640-9.
26. Shi Z, Bogaards SJP, Conijn S, et al. COVID-19 is associated with distinct myopathic features in the diaphragm of critically ill patients. BMJ Open Respir Res 2021;8:e001052.
27. Lewis P, O'Halloran KD. Diaphragm muscle adaptation to sustained hypoxia: lessons from animal models with relevance to high altitude and chronic respiratory diseases. Front Physiol 2016;7:623.
28. Deana C, Rovida S, Orso D, et al. Learning from the Italian experience during COVID-19 pandemic waves: be prepared and mind some crucial aspects. Acta Biomed 2021;92: e2021097.
29. Vetrugno L, Guadagnin GM, Barbariol F, et al. Ultrasound Imaging for diaphragm dysfunction: a narrative literature review. J Cardiothorac Vasc Anesth 2019;33:2525-36.
30. Poulard T, Bachasson D, Fossé Q, et al. Poor correlation between diaphragm thickening fraction and transdiaphragmatic pressure in mechanically ventilated patients and healthy subjects. Anesthesiology 2022;136:162-75.
31. Cammarota G, Rossi E, Vitali L, et al. Effect of awake prone position on diaphragmatic thickening fraction in patients assisted by noninvasive ventilation for hypoxemic acute respiratory failure related to novel coronavirus disease. Crit Care 2021; 25:305.
32. Hadda V, Raja A, Suri TM, et al. Temporal evolution of diaphragm thickness and diaphragm excursion among subjects hospitalized with COVID-19: a prospective observational study. Respir Med Res 2022;83:100960.
33. Hennigs JK, Huwe M, Hennigs A, et al. Respiratory muscle dysfunction in long-COVID patients. Infection 2022;50: 1391-7.
34. Schepens T, Fard S, Goligher EC. Assessing diaphragmatic function. Respir Care 2020;65:807-19.
35. Deana C, Vetrugno L, Cortegiani A, et al. Quality of life in COVID-related ARDS patients one year after intensive care discharge (Odissea Study): a multicenter observational study. J Clin Med 2023;12:1058.

***DIASUS Study Group**: Flavio Bassi, Francesco Meroi, and Daniele Orso (Department of Anesthesia and Intensive Care, Health Integrated Agency Friuli Centrale, Academic Hospital of Udine, Italy); Simone Bressan and Giulia Vaccher (Department of Medicine, University of Udine, Italy); Letizia Casarotto (Institute of Anatomic Pathology, Academic Hospital of Udine, Italy); Vincenzo Della Mea (Department of Mathematics, Computer Science and Physics, University of Udine, Italy); Lolita Fasoli (Division of Pediatrics, Academic Hospital of Udine, Italy); Francesca Stefani and Federico Barbariol (Department of Anesthesia and Intensive Care, Health Integrated Agency Friuli Centrale, Academic Hospital of Udine, Italy); Enrico Boero (Anesthesia and Intensive Care Unit, San Giovanni Bosco Hospital, Turin, Italy); Daniele Guerino Biasucci (Department of Clinical Science and Translational Medicine, 'Tor Vergata' University, Rome, Italy; Emergency Department, 'Tor Vergata' University Hospital, Rome, Italy; Catholic University of the Sacred Heart, Rome, Italy); Danilo Buonsenso (Department of Woman and Child Health and Public Health, Fondazione Policlinico Universitario A. Gemelli, Istituto di Ricovero e Cura a Carattere Scientifico (IRCCS), Rome, Italy; Centro di Salute Globale, Università Cattolica del Sacro Cuore, Roma, Italy); Luigi Pisani (Department of Intensive Care Medicine, Regional General Hospital F. Miulli, Acquaviva delle Fonti, Italy) Francesco Forfori (Department of Surgical, Medical, Molecular Pathology and Critical Care Medicine, University of Pisa, Italy); Federico Longhini (University of Magna Graecia, Catanzaro, Italy); Giuseppe Vetrugno (Fondazione Policlinico Universitario "A.Gemelli" IRCCS, Rome, Italy; Section of Hygiene, University Department of Life Sciences and Public Health, Università Cattolica del Sacro Cuore, Rome, Italy).

*Online supplementary material:*

*Supplementary Figure 1. Fast fiber content and their number relationship with mechanical ventilation. Fast myosin content showed a positive linear correlation with the percentage of controlled mechanical ventilation on total $LOS_{ICU}$ ($R^2$=0.446, p=0.006 as shown in panel A). On the opposite, their number decreased regarding the same ventilation parameters ($R^2$=-0.34, p=0.022 as shown in panel B).*

*Supplementary Table 1. Pre-existing conditions and relevant medical history.*

*Supplementary Table 2. Correlations between ventilatory parameters and anatomopathological findings.*